Chemistry | Lancaster University

« *Stimuli-responsive polymers for drug delivery* »

A dissertation submitted to

Lancaster University

for the degree of Master of Science (by research) in Chemistry

by

Vasileios Oikonomou, BSc

August 2018

ACKNOWLEDGEMENTS

This thesis was developed during my research at the Chemistry department of Lancaster University, UK, under the guidance of Dr. John G. Hardy, in which I owe gratitude for giving me the opportunity to work in such a challenging research field.

I would like to express my thanks to the technical personnel of the University for their help in the time it was needed and to all of my colleagues for helping me in everything that I needed and for the excellent working atmosphere and the good times spent together, specially I would like to thank Garry Harper and Mark Ashton for their help in every moment during this Thesis.

Finally, I am most grateful to my friends and of course to my parents, for their constant support, patience and encouragement throughout my thesis.

Vasileios Oikonomou

Lancaster, United Kingdom, August 2018

Table of Contents:

Article

Light-responsive polysaccharides for light-triggered drug delivery

Vasileios Oikonomou [1], and John G. Hardy [1,2,*]

[1] Department of Chemistry, Lancaster University, Lancaster, Lancashire, LA1 4YB, UK; v.oikonomou@lancaster.ac.uk (VO); j.g.hardy@lancaster.ac.uk
[2] Materials Science Institute, Lancaster University, Lancaster, Lancashire, LA1 4YB, UK.
* Correspondence: j.g.hardy@lancaster.ac.uk; Tel.: +44-1524-595-080

Abstract: Light responsive Hyaluronic acid-graft-(2-diazo-1,2-naphthoquinone) (HA-DNQ) was synthesized and characterized. The synthesis was achieved by the esterification of Hyaluronic acid with the photoactive unit of DNQ. Hyaluronic acid was chosen for its ability to potentially target cancer stem cells that overexpress CD44. Furthermore, the bioconjugate of hydrophilic Hyaluronic acid and hydrophobic DNQ is amphiphilic and can potentially assemble into micelles or other supramolecular assemblies and thereafter be used as a drug carrier. The release of which could happen upon irradiation at 365nm for a short period of time.

Keywords: polymers; photoactive; drug delivery.

1. Introduction

Devices that enable the precise spatiotemporal control of delivery of an active ingredient (e.g. agrochemical, detergent, drug, etc.) are of interest for a variety of applications. Of particular interest is the ability to control drug delivery, with the potential to maximise therapeutic effect and minimise drug side effects. Consequently, stimuli-responsive materials have been developed with such applications in mind, responding to a variety of triggers, such as light, magnetism, pH, temperature, and ultrasound.

Natural biopolymers such as polysaccharides and proteins are attractive for a number of biomedical/pharmaceutical applications (in part because they tend to be relatively non-immunogenic), e.g. drug delivery, scaffolds for tissue engineering, etc. Their inherent bioactivity offers opportunities for imparting interesting properties into biomaterials (e.g. cell adhesion/recognition, lubrication, mechanical properties) which has inspired researchers in academia and industry to develop a variety of biopolymer-based biomaterials.

Traditional drug delivery devices (creams, needles and tablets) tend to deliver a burst of a drug in a short space of time. Controlling the concentration of drug in the body is important because it is important to ensure the concentration of drug falls within the therapeutic window, above which it is toxic, and below which it is ineffective. Consequently, there has been significant research and development of drug delivery devices that control the concentration of drug for periods of time (e.g. implantable drug pumps). A variety of alternatives to pumps exist, often based on stimuli-responsive polymers with switchable properties in response to stimuli including pH, enzymes, ions, ultrasound, electricity and light.

Light-responsive drug delivery systems are popular in the clinic for the treatment of skin cancers using photodynamic therapy (employing photosensitisers to kill the cancerous cells), and light-responsive polymers are under development for the generation of materials (e.g. films, fibers, foams, gels and particulates) for delivering drugs to various tissue niches, particularly because drug delivery systems utilising light as an external trigger provide an

attractive means of tailoring the spatiotemporal release of a drug, with the ability to control the intensity, wavelength and duration of light exposure, enabling precise quantities of drug to be released on demand.

In this study, we report the preparation of light-responsive polymers suitable for drug delivery in response to irradiation with light (365 nm). The photoactive hyaluronic acid derivatives have the potential to target cancer stem cells that overexpress CD44 (hyaluronic acid binding protein)[1], and deliver drugs to those cells in response to the application of light which represents a useful strategy for on-demand drug delivery.

2. Materials and Methods

2.1. Materials

All materials were of analytical grade or higher and were used as supplied. Sodium hyaluronate (Mw = 1.5 – 2.2 million Da) was obtained from Acros Organics (Leicestershire, UK). 2-Diazo-1,2-naphthoquinone-5-sulfonyl chloride (sc-DNQ, 99%) was purchased by BOC Sciences (New York, USA) and was stored in the dark. Trimethylamine hydrochloride, triethylamine, nile red (98%), N,N-dimethylformamide (anhydrous 98%), and Dialysis tubing (Fisherbrand™ Regenerated Cellulose, MWCO 3500 Da) were purchased from Fisher Schientific (Loughborough, UK).

2.2. Methods

2.2.1. Conjugation of DNQ to Hyaluronic Acid – (HA-DNQ)

Hydrophilic hyaluronic acid was modified with hydrophobic and light-responsive sc–DNQ by adaptation of the literature[2,3]. 1.0 g (0.1 mmol) hyaluronic acid was dissolved in 150 ml of deionized (DI) water and triethylamine (1 ml, 7.4 mmol) trimethylamine hydrochloride (0,04 g, 0.74 mmol) were added. 2.0 g (7.4 mmol) sc-DNQ was diluted in 15 ml of DMF and added dropwise to the solution of hyaluronic acid. The reaction mixture was stirred in the dark (wrapped in aluminum foil) at room temperature for 48 hours. Product was purified by precipitation in acetone (four times), washing in cold methanol and soxhlet extraction with acetone to remove the excess sc-DNQ. The final product was dried under vacuum at room temperature for 24 h, yielding an orange solid (200 mg).

2.2.2. Preparation of HA-DNQ micelles and encapsulation of Nile Red

HA-DNQ (3mg) and Nile Red (0.06 mg) were dissolved in DMSO (1 ml). Water (1 ml) was added and the mixture was stirred for 6 h, after which it was dialyzed against deionized water (Fisherbrand™ Regenerated Cellulose, MWCO 3500 Da) for 72 hours.

2.2.3. Light irradiation setup

Light irradiation at various times was achieved using a ThorLabs LED DC4104 Driver system with a LED (365 nm) in a light proof container (outdoor plastic garden shedmanufactured by Keter).

2.2.4. Characterization

^{1}H & ^{13}C NMR spectra were recorded on a Bruker 400 Ultrashield Plus 400 MHz NMR spectrometer. For the ^{1}H NMR spectral splitting patterns the following notation is used: singlet (s), doublet (d), multiplet (m). Fourier transform infrared (FT-IR) spectroscopy was recorded on a Cary 630 FTIR (Agilent Technology) spectrophotometer at room temperature in the range of 500-4000 cm^{-1}. UV-vis spectra of Hyaluronic acid, sc-DNQ and the HA-DNQ were carried out with a UV-vis Thermo Scientific™ NanoDrop Spectrophotometer. UV-vis spectra for the

LED irradiation studies were recorded with a Cary 60 UV-Vis (Agilent Technologies) spectrophotometer in the range of 200-1080 nm.

3. Results

The bioconjugate of hyaluronic acid and DNQ (HA-DNQ) was prepared by modification of hydrophilic hyaluronic acid with the acid chloride sc-DNQ (Scheme 1

). The experimental conditions that were investigated are presented in Table 1. DNQ conjugation was confirmed both by ^{1}H NMR and FT-IR measurements.

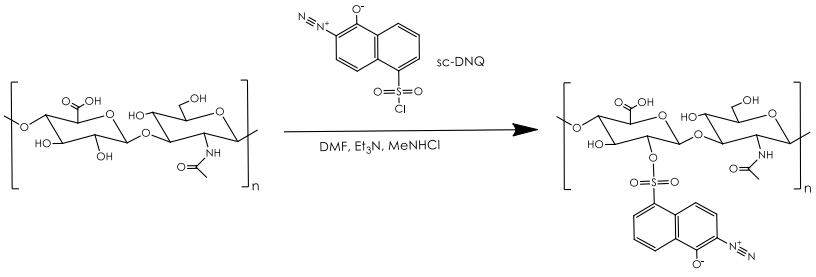

Scheme 1. Preparation of HA-DNQ.

Table 1 Formulations of HA-DNQ

Polymer	Weight ratio of HA:DNQ
HA-DNQ (Product 1)	1:1
HA-DNQ (Product 2)	1:2

Product 1 formed gel during the process of dilution for NMR characterization in D_2O (likely to be caused by supramolecular interactions between the hydrophobic photo responsive units displayed on the backbone of the HA (a process depicted in Scheme 2). Product 2 with a highaer ratio of DNQ was soluble in water and is likely to assemble into micelles because of its amphiphilic structures (a process depiteced in Scheme 2).

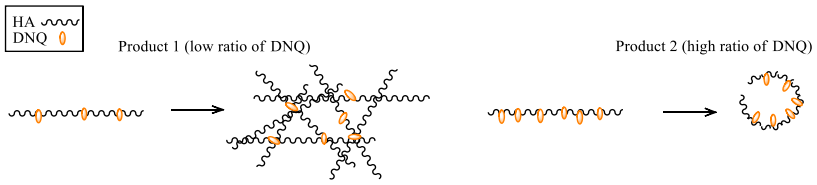

Scheme 2. Depiction of different formulations HA-DNQ

The ^{1}H-NMR spectrum of the unmodified hyaluronic acid is shown in Figure 2a, and is consistent with the literature,[4–6] the multiplets (m) at δ = 1.94 ppm are from the protons of N-$COCH_3$ groups. The ^{1}H-NMR spectrum of DNQ (Figure 2b) was consistent with the literature,[3] ^{1}H NMR for DNQ (D_2O, 400 MHz, 298 K) δ 8.38 ppm (m, 1H, Ar-H), 8.26 ppm (m, 1H, CH), 7.57 – 7.51 ppm (m, 1H, Ar-H), 7.38 ppm (m, 1H, Ar-H), 7.35 ppm (m, 1H, Ar-H). 10mg of the photo responsive unit was diluted in 500µl DMSO, then 5µl of that solution was added to an NMR tube with 500µl D_2O. The 1H NMR spectrum of HA-DNQ (Figure 2c) shows the successful conjugation of DNQ onto the hyaluronic acid. The FTIR spectra (Figure 3) of Hyaluronic acid, DNQ and HA-DNQ confirms the conjugation of DNQ to HA with the characteristic absorption peak of DNQ at ca. 2200 cm^{-1} that was

observed in the spectrum of HA-DNQ. UV-Vis spectroscopy also confirmed the successful conjugation of DNQ to HA (Figure 4) due to the characteristic absorption peak of the photo responsive unit at ca. 403nm.[3,7] For the UV-Vis measurements PBS was used as a solvent, the DNQ sample was diluted in DMSO first, similar as the preparation of the NMR sample (10 mg DNQ in 500 µl DMSO and 5 µl of that solution was diluted in 1000 µl of PBS). The photoresponsive characteristics of HA-DNQ are shown in Figure 5, with UV-Vis spectra recorded after various periods of irradiation at 365 nm with a LED.

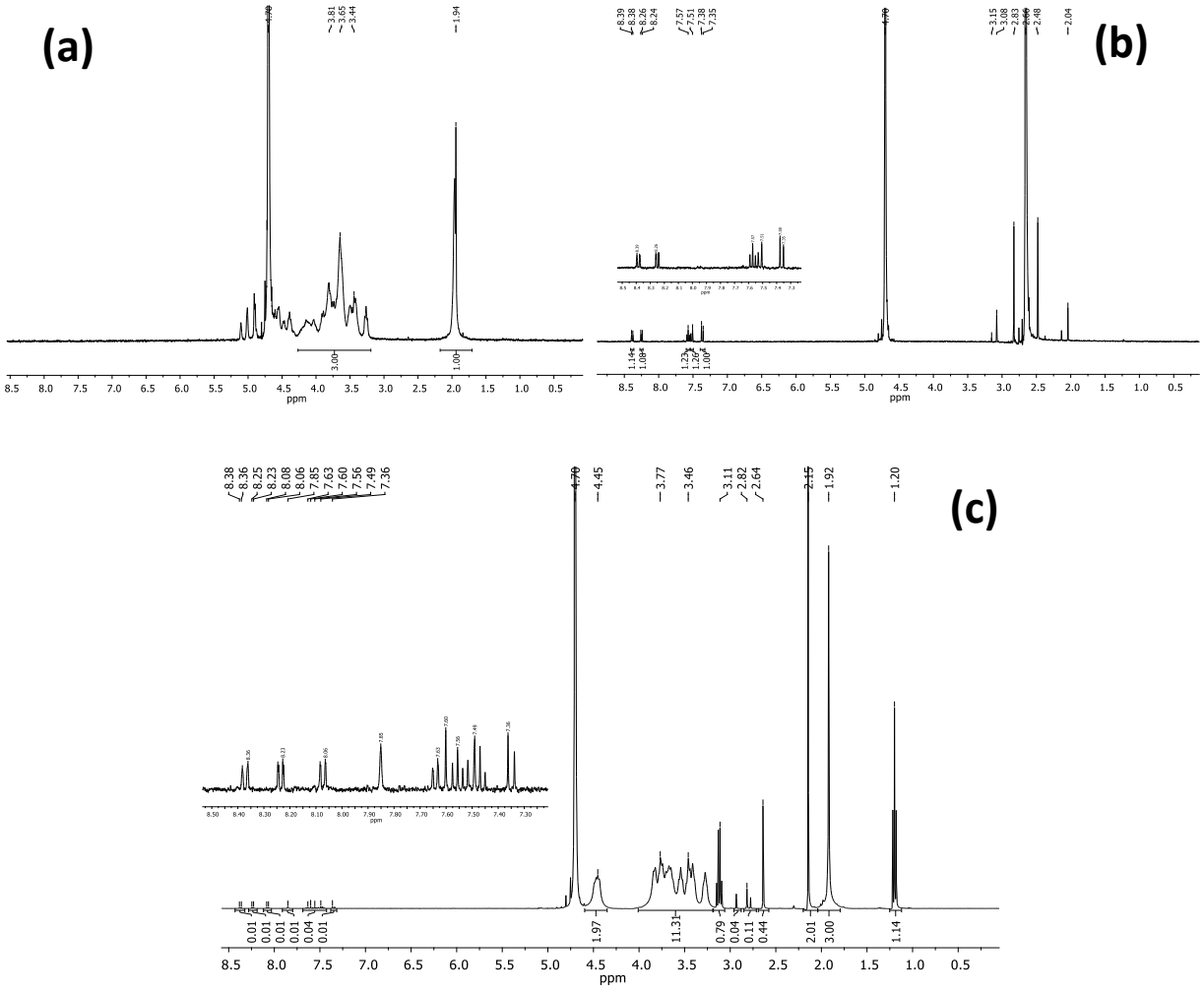

Figure 2. (a) ^{1}H-NMR spectrum of Hyaluronic acid **(b)** ^{1}H-NMR spectrum of DNQ **(c)** ^{1}H-NMR spectrum of HA-DNQ (Product 2)

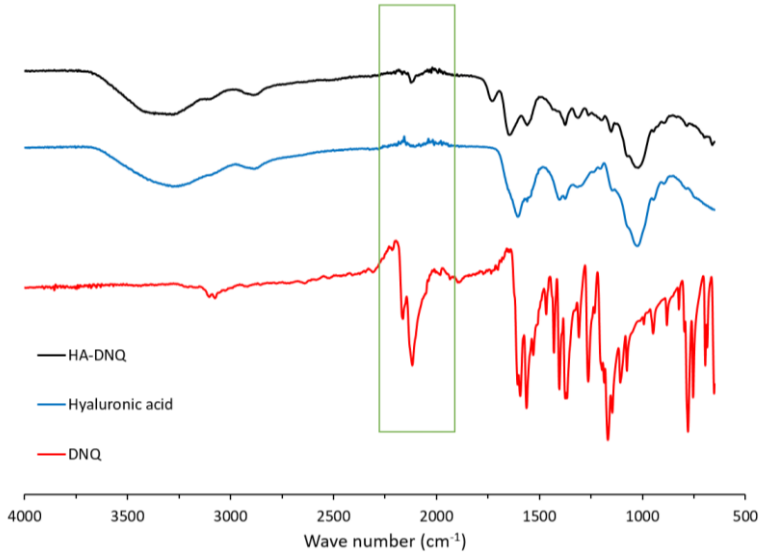

Figure 3. FT-IR spectra of HA-DNQ, hyaluronic acid and DNQ, highlighting the characteristic DNQ peak at 2118 cm^{-1}.

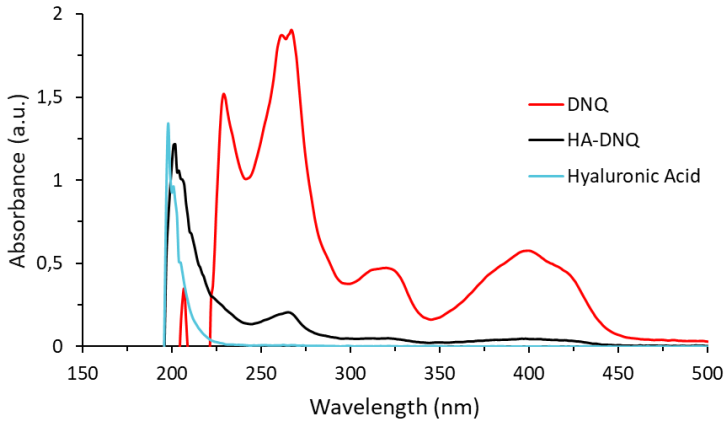

Figure 4. UV-Vis spectra of DNQ, HA-DNQ and hyaluronic acid standard.

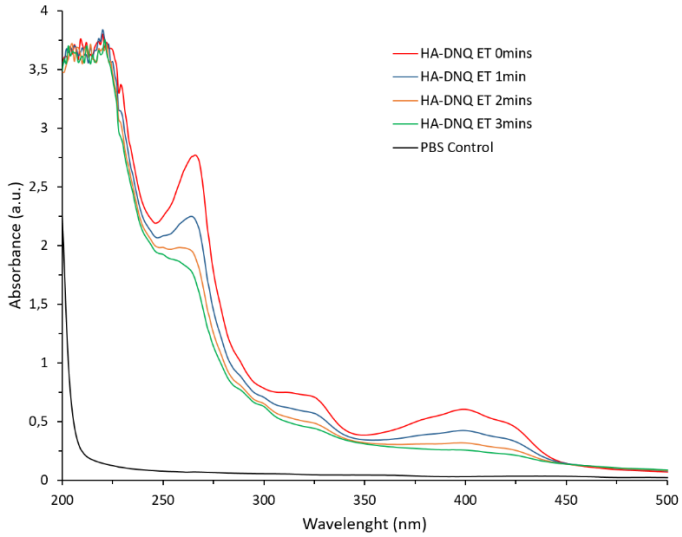

Figure 5. UV-Vis spectra of HA-DNQ (3.5 mg/ml in PBS) after irradiation with 365 nm light for various times (ET = elapsed time). .

4. Conclusion

HA is known to bind to cancer cells overexpressing CD44 and this has been used to target cancer cells for the delivery of a variety of drugs (including mitomycin C, cisplatin, quercetin doxorubicin and more) to various cell lines (231 Br, HT-29, MKN-45, and OE-21[8]).

The HA-DNQ was demonstrated to respond to light which shows promise for their ability to deliver drugs…XXX

Future work will include: DLS/zeta sizer, TEM, drug release studies in absence and presence of cells, and potentially in vivo.

Funding: This research received no external funding.

Acknowledgments: We thank Mark Ashton for assistance with synthesis and Garry Harper for assistance with setting up the light kit.

Conflicts of Interest: Declare conflicts of interest or state "The authors declare no conflict of interest.

References

1. Peach J., R., Hollenbaugh, D., Stamenkovic, I. & Aruffo, A. Identification of Hyaluronic Acid Binding Sites in the Extracellular Domain of CD44. *J. Cell Biol.* **122,** 257–264 (1993).

2. Yoshihiro Yoshida, Yoshiko Sakakura, Naoya Aso, Shin Okada, and Y. T. Practical and Efficient Methods for Sulfonylafion of Alcohols Using Ts(Ms)CI / Et3N and Catalytic Me3N.HCI as Combined Base: Promising Alternative to Traditional Pyridine. *Tetrahedron* **55,** 2183–2192 (1999).

3. Liu, G., Chen, C., Li, D., Wang, S. & Ji, J. Near-infrared light-sensitive micelles for enhanced intracellular drug delivery. *J. Mater. Chem.* 16865–16871 (2012). doi:10.1039/c2jm00045h

4. Bulpitt, P. & Aeschlimann, D. New strategy for chemical modification of hyaluronic acid : Preparation of functionalized derivatives and their use in the formation of novel biocompatible hydrogels. (1999).

5. Leach, J. B., Bivens, K. A., Patrick, C. W. & Schmidt, C. E. Hydrogels : Natural , Biodegradable Tissue Engineering Scaffolds. (2003). doi:10.1002/bit.10605

6. Neto, A. I. *et al.* Nanostructured Polymeric Coatings Based on Chitosan and Dopamine-Modifi ed Hyaluronic Acid for Biomedical Applications. 2459–2469 (2014). doi:10.1002/smll.201303568

7. Liu, J., Wei, Q. & Wang, L. An i-line molecular glass photoresist for high resolution patterning. *RSC Adv.* 25666–25669 (2013). doi:10.1039/c3ra45130e

8. Dosio, F., Arpicco, S., Stella, B. & Fattal, E. Hyaluronic acid for anticancer drug and nucleic acid delivery. *Adv. Drug Deliv. Rev.* **97,** 204–236 (2016).

Article

Light-responsive hydrogels for light-triggered drug delivery

Vasileios Oikonomou [1], and John G. Hardy [1,2,*]

[1] Department of Chemistry, Lancaster University, Lancaster, Lancashire, LA1 4YB, UK; v.oikonomou@lancaster.ac.uk (VO); j.g.hardy@lancaster.ac.uk (JGH)
[2] Materials Science Institute, Lancaster University, Lancaster, Lancashire, LA1 4YB, UK.
* Correspondence: j.g.hardy@lancaster.ac.uk; Tel.: +44-1524-595-080

Abstract:

Biocompatible light-responsive hydrogels for drug delivery have been investigated. Methacrylate-based hydrogels and a photolabile crosslinker have been prepared from commercially available chemicals. The drug release studies of a variety of model drugs has been tested, as well as the photoresponsive properties of the crosslinker by irradiation at 365 nm with an LED. In order to increase the hydrophilicity of the polymer backbone and achieve better drug release results, the hydrogels were re-engineered with PEG derivatives.

Keywords: light; photoactive; polymers; drug delivery

1. Introduction

Devices that enable the precise spatiotemporal control of delivery of an active ingredient (e.g. agrochemical, detergent, drug, etc.) are of interest for a variety of applications. Of particular interest is the ability to control drug delivery, with the potential to maximise therapeutic effect and minimise drug side effects[1]. Consequently, stimuli-responsive materials have been developed with such applications in mind, responding to a variety of triggers, such as light, magnetism, pH, temperature, and ultrasound.

Hydrogels based on 2-hydroxyethyl methacrylate (HEMA) and dimethacrylate-based crosslinkers have been in use for several decades, particularly for contact lenses, and hydrogels based on poly(ethylene glycol) (PEG) are attractive for a number of biomedical/pharmaceutical applications[2]. Polymer-based hydrogels with switchable properties have potential for the development of stimuli-responsive hydrogels that may find applications as sensors, switches, artificial muscles and drug delivery devices.

The mechanical properties of hydrogels dictate their potential for specific applications, with tissue scaffolds ideally having mechanical properties similar to the tissue in which they are to be implanted, and coatings for biomedical devices needing to adhere on the device and remain attached once inside the body (particularly as they may also serve to act as a reservoir for bioactive molecules). Mechanically robust stimuli-responsive coatings for medical devices are an attractive concept, potentially allowing the user to precisely control the level of drug in the body and treat the condition when and where it is most efficacious. Drug delivery systems utilising light as an external trigger provide an attractive means of tailoring the spatiotemporal release of a drug, with the ability to control the intensity, wavelength and duration of light exposure, enabling precise quantities of drug to be released on demand. O-nitrobenzyl derivatives have been used to prepare photosensitive drug-conjugates (e.g. photoactive esters) and photocleavable hydrogels. Here report the preparation of a novel photoactive crosslinker that should be capable of use in photoactive hydrogels for the delivery of drugs in response to irradiation with light (365 nm, or 730 nm 2-photon source).

2. Materials and Methods

2.1. Materials

All materials were of analytical grade or higher and were used as supplied from Sigma-Aldrich (Dorset, UK) unless otherwise stated.

2.2. Methods

2.2.1. Synthesis of Photocleavable Crosslinker

2-nitro-p-xylylene glycol (5 g, 27 mmol, purchased from TCI) and dichloromethane (150 ml) were placed in a round bottomed flask (250 ml) with a stirrer bar, and the mixture was cooled to 0 ^{o}C using an ice bath under an inert atmosphere (N_2). Once cooled, triethylamine (8 ml) and methacryloylchloride (7 g, 6.5 ml, 73 mmol) were added and the solution was stirred for 24h, allowing it to warm to room temperature. After 24h an aqueous extraction was used to remove the water soluble byproducts, followed by extraction with saturated aqueous sodium chloride. The organic phase was dried over $MgSO_4$ and the volatiles were removed by rotary evaporation. The purification was achieved by silica column chromatography (EtOAc/Hexane 1:1 as eluent), and the residue was dried in a vacuum oven at room temperature. This process yielded a yellow solid (4.280 g). ^{1}H NMR ($CDCl_3$, 400 MHz), δ 2.01 ppm (s, methacrylate CH_3, 6H), 5.67 ppm (methacrylate, 2H), 6.21 ppm (methacrylate, 2H), 7.63 ppm (m, Ar-H, 1H), 7.66 ppm (m, Ar-H, 1H), 8.14 (m, Ar-H, 1H).

2.2.2. Synthesis of Model Photocleavable Crosslinker

2-nitro-p-xylylene glycol (5 g, 27 mmol) and dichloromethane (150 ml) were placed in a round bottomed flask (250 ml) with a stirrer bar, and the mixture was cooled to 0 ^{o}C using an ice bath, under an inert atmosphere (N_2). Once cooled, triethylamine (8 ml) and acetyl chloride (5.25 g, 73 mmol) were added and the solution was stirred for 24h, allowing it to warm to room temperature. After 24h an aqueous extraction was used to remove the water soluble byproducts, followed by extraction with saturated aqueous sodium chloride. The organic phase was dried over $MgSO_4$ and the volatiles were removed by rotary evaporation. The purification was achieved by silica column chromatography (EtOAc/Hexane 1:1 as eluent), yielding a residue that was dried in a vacuum oven at room temperature. This process yielded a viscous yellow liquid (1.0 g). ^{1}H NMR ($CDCl_3$, 400 MHz), δ 2.17 ppm (s, methacrylate CH_3, 6H), 5.48 ppm (methacrylate, 2H), 6.21 ppm (methacrylate, 2H), 7.58 ppm (m, Ar-H, 1H), 7.65 ppm (m, Ar-H, 1H), 8.10 (m, Ar-H, 1H).

2.2.3. HEMA-MAA Hydrogel Preparation and Drug Loading Procedure

Hydroxyethylmethacrylate (HEMA) (75 ml), methacrylic acid (MAA) (75 ml) and FITC-Dextran derivatives (1.5 mg) were placed in a 250 round bottomed flask and stirred for 48h for Dextran to be dissolved. A portion of this mixture was then placed in a beaker with a crosslinker, either the non-photolabile crosslinker ethylene glycol dimethacrylate (EGDMA) or the photolabile crosslinker and the thermal initiator benzoylperoxide (BPO). The mixture was stirred in the dark until the BPO was fully dissolved (ca. 10 mins) the final mixture was injected into a plate mould to prepare gels of 1 mm thickness as described in the literature.[3] The injected samples were placed in an oven and polymerised at 90 ^{o}C for 3 hours, after which they cooled to room temperature and washed extensively with DI water for 7 days, changing the water every few hours to remove any excess of monomer. The gels were stored in the dark while washing and prior to use.

Photoactive and non-photoactive gels were synthesised with 1% and 5% of crosslinkers respectfully. For the non-photoactive gels (1%): HEMA (5 ml), MAA (5 ml), EGDMA (0.1 ml), BPO (0,04 g). Non-photoactive gels (5%): HEMA (5 ml), MAA (5 ml), EGDMA (0.5 ml), BPO (0,04 g). Photoactive gels (1%): HEMA (5 ml), MAA (5 ml), photolabile crosslinker (0.1 g), BPO (0,04 g). Photoactive gels (5%): HEMA (2.5 ml), MAA (2.5 ml), photolabile crosslinker (0.25 g), BPO (0,02 g).
The FITC-Dextran that were used had the molecular weights of 10 kDa, 40 kDa, 70 kDa and 500 kDa, by having four molecular weights in Dextran and two different ratios in the two crosslinkers the gels, sixteen different formulations were prepared for testing.

2.2.4. PEGDA Hydrogel Preparation

A more hydrophilic polymer backbone was used for the second gel preparation. Poly(ethylene glycol) diacrylates of 6 kDa and 10 kDa Mw were used for this synthesis. PEGDA was in a glass vial with a stirrer and placed on a hotplate at 60 ^{o}C to melt. Once the diacrylate was melted and a viscous solution was formed a non-photolabile crosslinker (EGDMA) was added to the vial and left to homogenize. After the mixing of the two substances the thermal initiator was added, by the time BPO was dissolved the solution was injected in circular molds of 5 mm diameter and 1 mm height. The molds were placed in the oven at 90 ^{o}C for 3 hours. After this period the molds were cooled to room temperature and washed extensively with DI water for 3 days to remove any non crosslinked components.

2.2.5. Irradiation apparatus

To investigate the photocleavage characteristics of the photolabile crosslinker and the model crosslinker, LED irradiation at varying time points was achieved using a ThorLabs LED DC4104 Driver system with LEDs (365 nm).

2.2.6. Characterization

^{1}H NMR spectra were recorded on a Bruker 400 Ultrashield Plus 400 MHz NMR spectrometer. For the ^{1}H NMR spectral splitting patterns the following notation is used: singlet (s), doublet (d), multiplet (m). Fourier transform infrared (FT-IR) spectroscopy was recorded on a Cary 630 FTIR (Agilent Technology) spectrophotometer at room temperature in the range of 500-4000 cm^{-1}. UV-vis spectra for the LED irradiation studies were recorded with a Cary 60 UV-Vis (Agilent Technologies) spectrophotometer at room temperature within a range of 200-1080 nm. Fluorescence spectra were recorded using a FLUOstar Omega plate reader (BMG LABTECH, Germany)

2.2.7. Swelling Tests

The swelling ration based on mass (Q_M) was determined experimentally on the PEG diacrylate gels[4]. The cylindrical gel disks with 5 mm diameter and 1 mm thickness were dried in vacuum oven until a constant dry mass (M_d). The swelling ration based on mass (Q_M) was then determined by dividing the swelled mass in the solvent by the dry mass:

$$Q_M = M_s/M_d$$

This was used to calculate the volumetric swelling ratio[5], Qv. In which ρ_p is the mass-weighted average density of the dry polymers (pHEMA = 1.15 g cm^{-3}; pMAA = 1.285 g cm^{-3}) and ρ_s is the density of the solvent (either 0.789 g cm^{-3} for ethanol or 1 g cm^{-3} for PBS).

$$Qv = 1 + \frac{\rho_p}{\rho_s}(Q_M - 1)$$

2.2.8. Drug Delivery

HEMA-MAA gel disks were cut with medical biopsy punches with a diameter of 4mm and placed in 96 well plates with 150 μl of PBS. Samples were incubated in PBS for 30 mins in order to equilibriate and then optionally irradiated with light at 365 nm using a 5 W Hg discharge UV-A lamp at a height of 10 cm above the samples, shielded to prevent interference from ambient light. The samples were irradiated for 1 hour after which they placed in the dark (control samples were maintained in the dark for the duration of the experiment)[6]. The release medium was transferred to another 96 well plate for spectrophotometric analysis. Fluorescence spectra were recorded for 1 hour, 2 hours, 3 hours and 4 hours of irradiation as well as the control samples in the dark.

3. Results

3.1. Preparation and Characterization of Photolabile Crosslinker

A photocleavable crosslinker was prepared by esterification of 2-nitro-p-xylylene glycol with methacryloyl chloride (Scheme 1) and purified by column chromatography. The ^{1}H-NMR spectrum of the photolabile crosslinker is depicted at Figure 1. ^{1}H NMR ($CDCl_3$, 400 MHz), δ 2.01 ppm (s, methacrylate CH_3, 6H), 5.67 ppm (methacrylate, 2H), 6.21 ppm (methacrylate, 2H).

The FTIR spectrum (Figure 2) depicts the presence of the ester with the characteristic absorption peak at around 1720 cm^{-1} and the peak of the aromatic amine at around 1300 cm^{-1}.

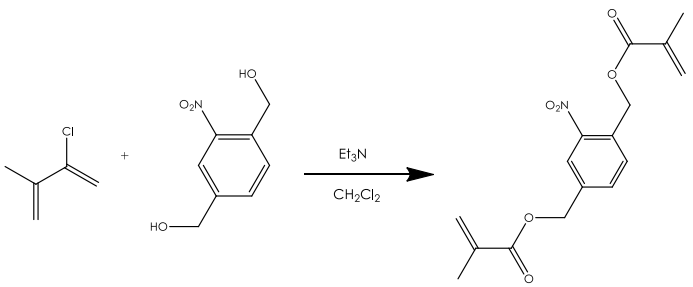

Scheme 1. Synthesis of Photolabile crosslinker

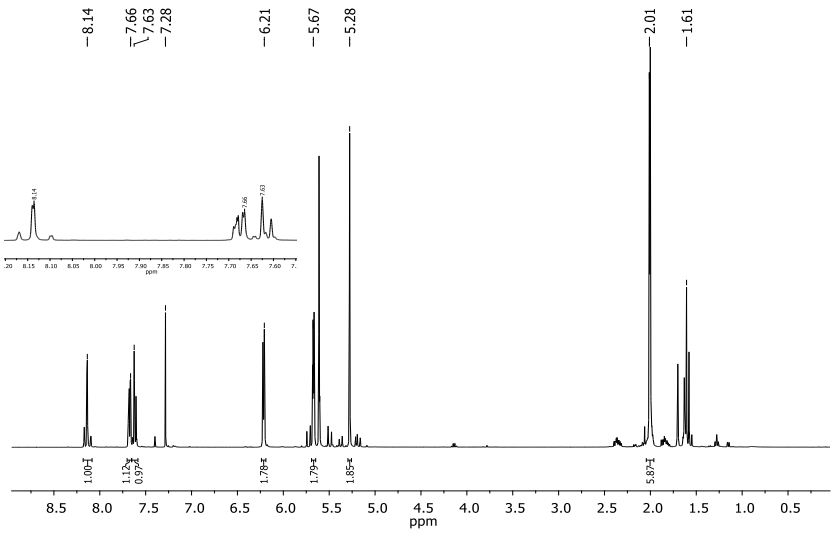

Figure 1. ^{1}H NMR of photolabile crosslinker.

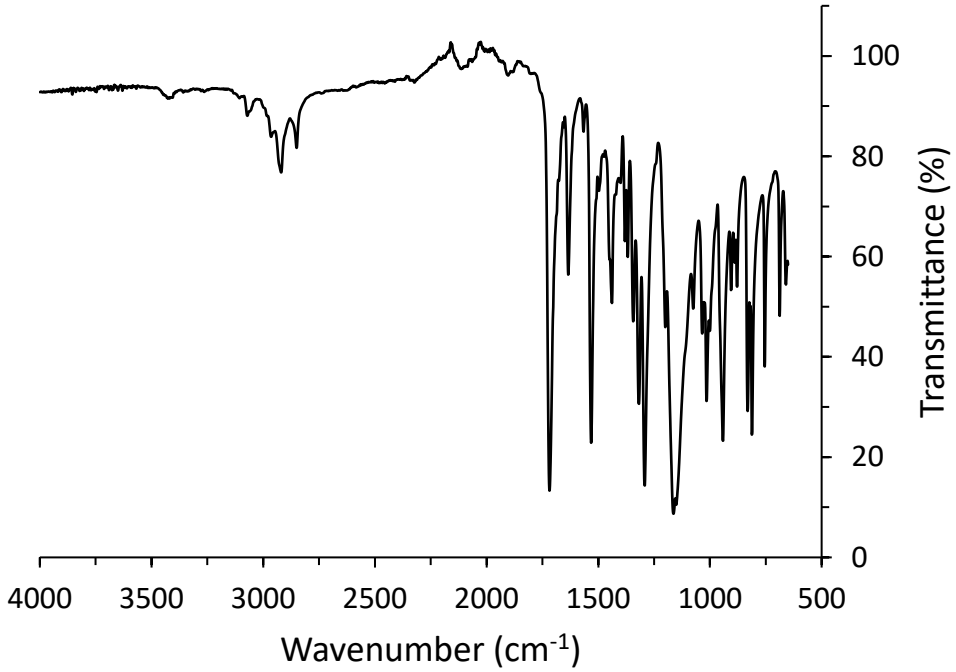

Figure 2. FT-IR of the photolabile crosslinker.

3.2. Preparation and Characterization of HEMA:MAA gels

Hydrogels composed of HEMA, MAA, and either a non-photolabile crosslinker (EGDMA) or the photolabile crosslinker at a concentration of either 1% or 5% by weight were prepared (Figure 3, Table 1). The swelling ratio based on mass (Q_M) was determined experimentally, enabling the calculation of the volumetric swelling ratio (Q_V) of the gels in PBS (Table 1). This enables determination of the volume of solvent in disks of gel (1 mm height and 5 mm diameter) which dictates the amount of drug the gel can entrap (Table 1). The gels prepared with a higher concentration of photolabile crosslinker swelled less than those with lower concentrations of crosslinker, as evidenced by values for Q_M, Q_V, and the volume of solvent in

the gels is correspondingly higher for the gels with 1% photoactive crosslinker than for those with 5% photoactive crosslinker (Table 2).

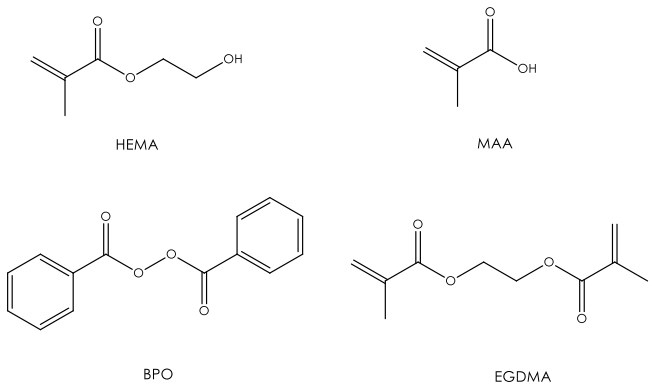

Figure 3. Chemicals used for the preparation of gels

Table 1. Formulations of HEMA:MAA gels used with encapsulated Dextran of 10k, 40k, 70k and 500k Da.

	Non-photoactive gels			Photoactive gels	
	1% crosslinker	5% crosslinker		1% crosslinker	5% crosslinker
EGDMA	0.1 ml	0.5 ml	Photocleavable Crosslinker	0.1 g	0.25 g
MAA	5 ml	5 ml	MAA	5 ml	2.5 ml
HEMA	5 ml	5 ml	HEMA	5 ml	2.5 ml
BPO	0.04 g	0.04 g	BPO	0.04 g	0.02 g

Table 2. Gel properties when swollen in PBS. Gels analysed were discs 5 mm in diameter and 1 mm thick.

Property	**Non-photoactive crosslinker (1%)**	**Non-photoactive crosslinker (5%)**	**Photoactive crosslinker (1%)**	**Photoactive crosslinker (5%)**
Q_M	2.21 ± 0.12	2.36 ± 0.09	3.16 ± 0.22	2.36 ± 0.16
Q_V	2.56 ± 0.14	2.75 ± 0.11	3.78 ± 0.26	2.75 ± 0.19
Volume of solvent in disc of gel (μl)	19.85 ± 1.78	28.31 ± 1.08	31.18 ± 2.17	26.3 ± 1.83

3.3. Drug Loading and Controlled Release

Drug loading was achieved by thermally crosslinking the gel formulations loaded with the model drugs (FITC-Dextran derivatives with molecular weights of 10 kDa, 40 kDa, 70 kDa and 500 kDa) release studies were not successful, which is possibly due to the mesh sizes of the gels impeding diffusion of the polymeric drugs in/out of the gels, or the poor responsiveness of the crosslinker to irradiation with light at 365 nm. To test the latter hypothesis the photocleavage characteristics of the crosslinker were assessed for the total duration of 30 minutes irradiation with a 365 nm LED, with no indication of successful photocleavage from the UV-Vis spectrum (Figure 4).

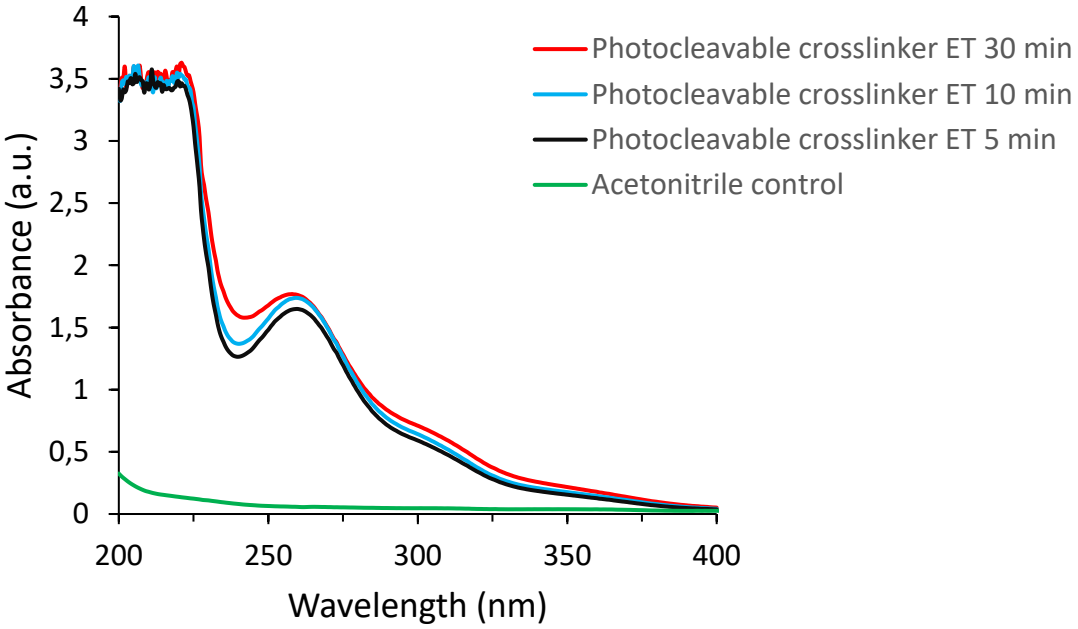

Figure 4. UV-Vis spectra of photocleavable studies in varying time periods (ET = elapsed time). Concentration of photolabile crosslinker is 0.15 mg/ml Acetonitrile.

3.4. Preparation and Characterization of Model Crosslinker

The model crosslinker (Scheme 2) was synthesized to investigate the photocleavage of the previously mentioned crosslinker compound (Scheme 1). The ^{1}H-NMR spectrum of the model crosslinker is presented in Figure 5. ^{1}H NMR ($CDCl_3$, 400 MHz), δ 2.17 ppm (s, methacrylate CH_3, 6H), 5.48 ppm (methacrylate, 2H), 6.21 ppm (methacrylate, 2H), 7.58 ppm (m, Ar-H, 1H), 7.65 ppm (m, Ar-H, 1H), 8.10 (m, Ar-H, 1H). The FTIR spectrum (Figure 6) shows an ester peak at around 1700 cm^{-1}.

The irradiation studies with 365 nm LED delivered positive photocleaving data, presented in the UV-Vis spectra (Figure 7 and Figure 8) with a total elapsed time of 10 minutes of irradiation. Even after 3 minutes of irradiation, there was clear evidence of photocleavage of the model crosslinker (Figure 8). This motivated us to attempt to form photoactive hydrogels by esterifying this diol and polyethyleneglycol diacids.

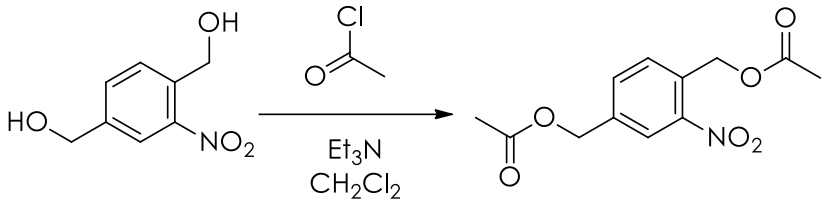

Scheme 2. Synthesis of the model crosslinker

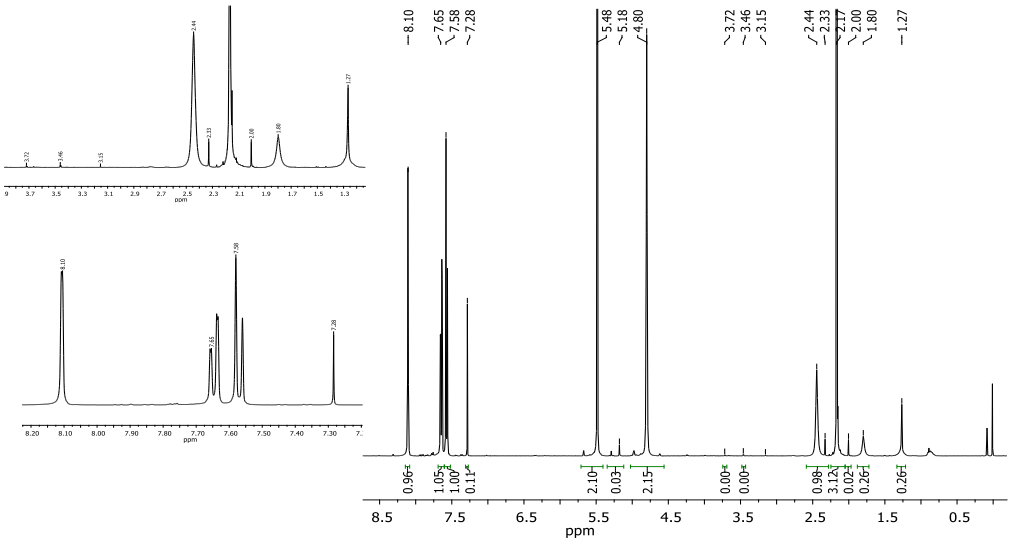

Figure 5. [1]H NMR of model crosslinker.

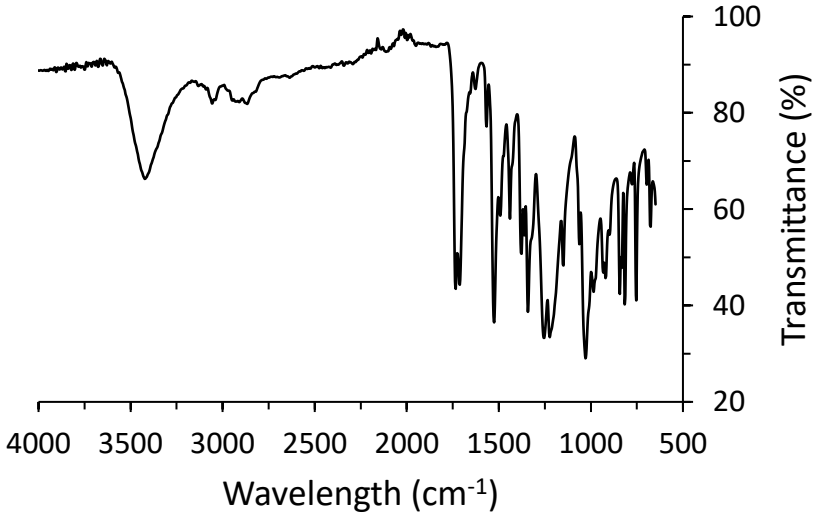

Figure 6. FT-IR of model crosslinker.

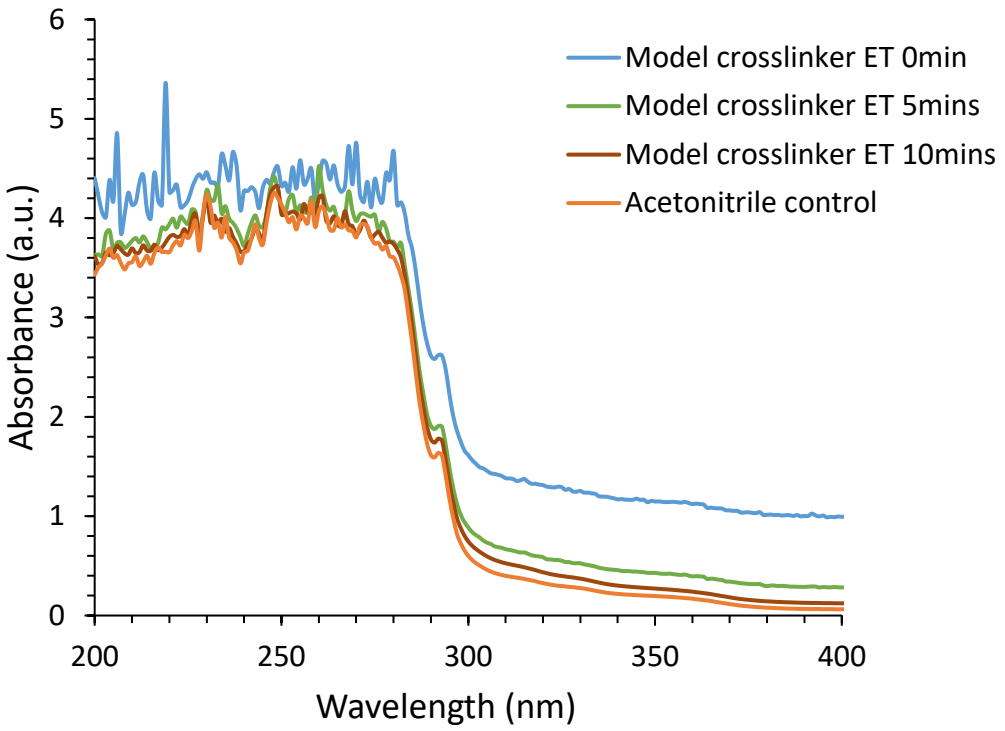

Figure 7. UV-Vis spectra of photocleavage studies at varyious time points (ET = elapsed time). The concentration of model crosslinker is 0.3 mg/ml Acetonitrile.

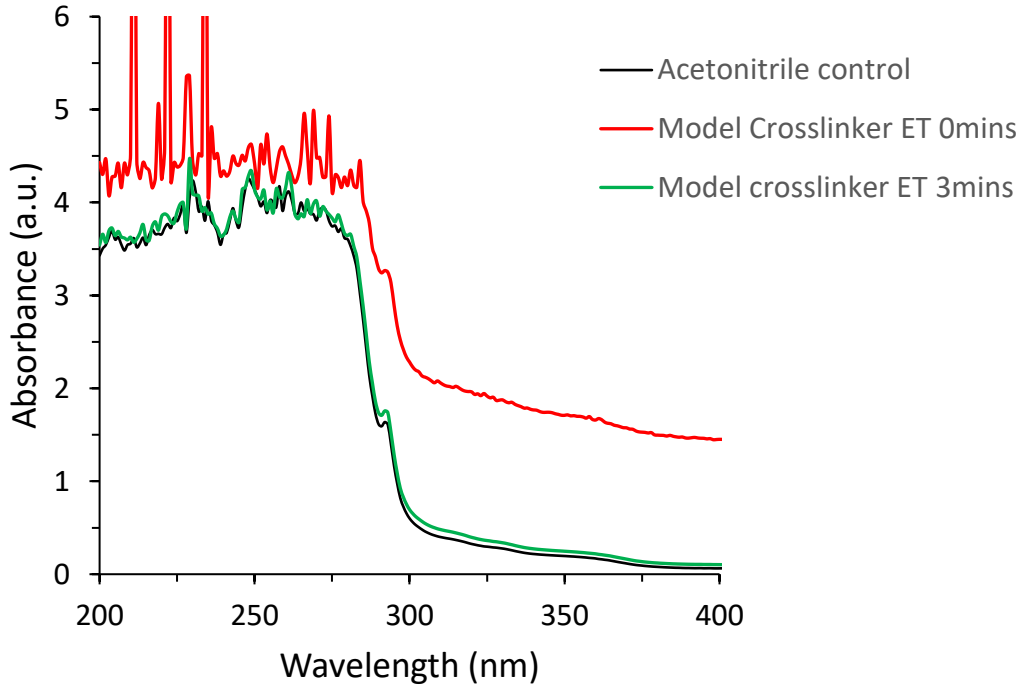

Figure 8. UV-Vis spectra of photocleavage studies at various time points (ET = elapsed time). The concentration of model crosslinker is 0.25 mg/ml Acetonitrile

3.5. Preparation and Characterization of non-photoactive PEGDA gels

A variety of different non-photoactive PEG gels were prepared to assess their handling properties, as robust and easily handleable gels are more useful for clinical applications (e.g. as medical device coatings), the results of which are displayed in Table 3. These tests suggest that the robust gels could be used as prototype formulations for the development of photoactive gels based on a combination of the photoactive diol and PEG diacid derivatives which will be a focus of future researchers in the Hardy lab.

Table 3. Formulations of PEGDA gels and comments for their mechanical properties

	PEGDA 6k Mw	PEGDA 10k Mw	BPO	EGDMA	DMSO	PEGDA 575 Mw	Comments
Gel 1	100 mg	-	4 mg	100 µl	500 µl	-	Pasty
Gel 2	100 mg	-	4 mg	100 µl	-	500 µl	Brittle
Gel 3	50 mg	-	4 mg	500 µl	-	-	Brittle
Gel 4	100 mg	-	4 mg	500 µl	-	-	Brittle
Gel 5	100 mg	-	4 mg	100 µl	-	-	Brittle
Gel 6	500 mg	-	4 mg	100 µl	-	-	Robust
Gel 7	50 mg	-	4 mg	500 µl	500 µl	-	Brittle
Gel 8	100 mg	-	4 mg	500 µl	500 µl	-	Brittle
Gel 9	100 mg	-	4 mg	100 µl	500 µl	-	Brittle
Gel 10	500 mg	-	4 mg	100 µl	500 µl	-	Robust
Gel 11	-	500 mg	4 mg	100 µl	-	-	Robust
Gel 12	-	500 mg	4 mg	100 µl	500 µl	-	Robust

4. Conclusions

While the methacrylated ONB compound first investigated for use as a crosslinker was inactive, the simpler model photoreactive crosslinker was active. It is possible to generate robust PEG-based gels, and some of the formulations tested will be used as prototype formulations for the development of photoactive gels based on a combination of the

photoactive diol and PEG diacid derivatives which will be a focus of future researchers in the Hardy lab.

Funding: This research received no external funding.

Acknowledgments: We thank Mark Ashton for assistance with synthesis and Garry Harper for assistance with setting up the light kit.

Conflicts of Interest: The authors declare no conflict of interest.

References

1. Feksa, L. *et al.* in *Nanostructures for the Engineering of Cells, Tissues and Organs* 403–438 (2018). doi:10.1016/B978-0-12-813665-2.00011-9

2. Venkatesh, S., Saha, J., Pass, S. & Byrne, M. E. Transport and structural analysis of molecular imprinted hydrogels for controlled drug delivery. *Eur. J. Pharm. Biopharm.* **69,** 852–860 (2008).

3. Brady, C. *et al.* Novel Porphyrin-Incorporated Hydrogels for Photoactive Intraocular Lens Biomaterials. 527–534 (2007). doi:10.1021/jp066217i

4. Hardy, J. G., Lin, P. & Schmidt, C. E. Biodegradable hydrogels composed of oxime crosslinked poly (ethylene glycol), hyaluronic acid and collagen : a tunable platform for soft tissue engineering. *J. Biomater. Sci. Polym. Ed. Biomater. Sci.* **26,** 143–161 (2015).

5. Krevelen, V. Properties of Polymers. *Elsevier* 341–344 (1990).

6. Donnelly, L. *et al.* Photochemically Controlled Drug Dosing from a Polymeric Scaffold. 1469–1476 (2017). doi:10.1007/s11095-017-2164-9

Communication

Silk-based biomaterials for bone tissue engineering: a promising dental stem cell niche.

Vasileios Oikonomou [1], and John G. Hardy [2,*]

[1] Department of Chemistry, Lancaster University, Lancaster, Lancashire, LA1 4YB, UK; v.oikonomou@lancaster.ac.uk (VO); j.g.hardy@lancaster.ac.uk (JGH)
[2] Materials Science Institute, Lancaster University, Lancaster, Lancashire, LA1 4YB, UK.
* Correspondence: j.g.hardy@lancaster.ac.uk; Tel.: +44-1524-595-080

Abstract:

Silk fibroin from *Bombyx mori* cocoons can be used as a biomaterial for a variety of biomedical applications. In the present research report, porous fibroin scaffolds have been prepared and characterized their chemical properties. The processing method that was used in this research can produce 3D scaffolds of different dimensions to suit a variety of applications. In vitro and in vivo studies are ongoing from the group of Xuebin Yang at the University of Leeds for dental applications.

Keywords: tissue scaffolds; tissue engineering; biomaterials; silk; stem cells; dental.

1. Introduction

Bone tissues are complex hierarchically ordered structures, which play a vital role in our lives. Bones are composite materials containing both vascularized soft tissue and collagen-/hydroxyapatite-rich hard tissue. There is a huge market need for biomaterials that facilitate bone tissue regeneration to treat conditions/disorders that require surgical intervention which are particularly important in societies with ageing populations.

A wide variety of materials have been investigated for their potential application in bone repair and regeneration, including inorganic materials (ceramics, glasses, metals), or polymers (synthetic or natural biopolymers). Biopolymer-based tissue scaffolds (e.g. those composed of polysaccharides and proteins) are particularly interesting because of their inherent biodegradability and bioactivity.

Natural silk proteins produced by silkworms (e.g. *Bombyx mori*) are under investigation for a variety of biomedical applications (e.g. bioactuators, drug delivery, optoelectronics), particularly as tissue scaffolds for tissue engineering with encouraging results both in vitro and in preclinical studies. Each tissue niche has different chemical compositions, mechanical properties and hierarchically organized topographies, and *B. mori* silk fibroin-based tissue scaffolds with biomimetic topographies have been developed for most common tissue niches (e.g. bone, muscle, nerve and skin).

An increasingly popular approach to enabling tissue regeneration is the development of scaffolds that enable the behavior of the cells to be controlled in a rational fashion in response to chemical or physical cues (e.g. drugs, electricity, mechanical forces). Such pro-regenerative tissue scaffolds have been developed for various tissue niches including bone, muscle, nerve and skin.

The concept of using silk-based materials as bone tissue scaffolds was studied extensively by Kaplan and coworkers, who have reported various materials morphologies (e.g. films,

fibers, foams, hydrogels) can enhance the differentiation of stem cells towards osteogenic outcomes. The first example of pro-regenerative silk-based tissue scaffolds employing electricity as a pro-regenerative cue was reported by Hardy and Kaplan,[1–3] wherein conducting polymers enhanced the differentiation of human mesenchymal stem cells towards osteogenic outcomes.

Mechanical forces are frequently exerted on bones and they are known to influence stem cell differentiation. Research in this area is a focus of the group of Xuebin Yang at the University of Leeds. Here we describe the preparation of 3D silk foams for potential use as instructive bone tissue scaffolds that enable mechanical stimulation of stem cells. The ability of these scaffolds to enhance bone tissue formation via in vitro and in vivo studies is currently being assessed by the group of Xuebin Yang (specifically for dental applications).

2. Materials and Methods

2.1. Materials

All materials were of analytical grade or higher and were used as supplied from Sigma-Aldrich (Dorset, UK) unless otherwise stated. Degummed *Bombyx mori* silk fibers (throwsters waste) were purchased from Amazon.co.uk.

2.2. Methods

2.2.1. Preparation of silk fibroin solution

B. mori silk fibers (30 g) were in a 1 L glass bottle and $CaCl_2$, H_2O and EtOH were added in a mole ratio of 1:8:2 (222 g, 272 ml, 237.2 ml).[4] The solution was stirred until the fibers were fully dissolved (c.a. 30 min) after which the solution was passed over a glass frit filter to remove any solid debris. The filtered mixture dialysed against deionized (DI) water (Spectra/Por®, 10k MWCO purchased by Spectrum Labs) for 3 days, after which it was centrifuged twice (8000 r.p.m., ca. 15.942 g) at 4°C for 20 min each time.[5] After centrifugation the mixture was upconcentrated by dialysis in a solution of 10% w/v PEG 10k Mw in deionized water for 24 hours to achieve the needed concentration. The silk content of the final solution was assessed by dry weight analysis, and the solution and was stored at 4°C.

2.2.2. Preparation of silk fibroin foams/scaffolds/sponges

Fine salt particles (400 μm, sieves were purchased by Advantech Manufacturing Inc.) were placed in a glass petri dish with a diameter of 14 cm and height of 2 cm (ca. 150 g of salt). The fibroin solution was carefully poured into the petri dish mould until all of the salt was immersed, after which the petri dish was covered and left for 2 days at room temperature for β-sheet formation to occur and the silk to gelation. Once the silk was gelled, the mold with the gel were immersed in DI water to extract the salt, changing the water every 2 hours for 2 days (after the first day the samples were able to be removed from the petri dish mold which helped homogeneously remove the salt).Cylindrical tissue scaffolds with diameters of 4 mm were cut out of the silk foams using medical autopsy punches, after which the scaffolds were immersed in ethanol and dried overnight in a fume hood and thereafter stored at room temperature.

2.2.3. Characterization

Fourier transform infrared (FT-IR) spectroscopy was recorded on a Cary 630 FTIR (Agilent Technology) spectrophotometer at room temperature between 500-4000 cm^{-1}. The XRD spectrum of a powdered fibroin scaffold was recorded with a Rigaku SmartLab Powder XRD. TGA analysis was performed with a Netzsch STA449C TGA-DSC system. Solid State NMR

spectrum was acquired with a Bruker AVANCE III HD 700WB ssNMR. MicroCT scans were recorded with a Bruker Skyscan X-Ray microtomographer.

3. Results

3.1. Fourier-transform infrared spectroscopic analysis of the silk fibroin scaffolds

The FTIR spectra (Figure 1) of the silk fibroin scaffold depict the characteristic absorption peaks around 1617 cm^{-1} from the peptide backbone of the amide I (C=O stretching), at around 1510 cm^{-1} for amide II (N-H bending) and at around 1223 and 1438 cm^{-1} to amide III (C-N stretching).[4,6,7]

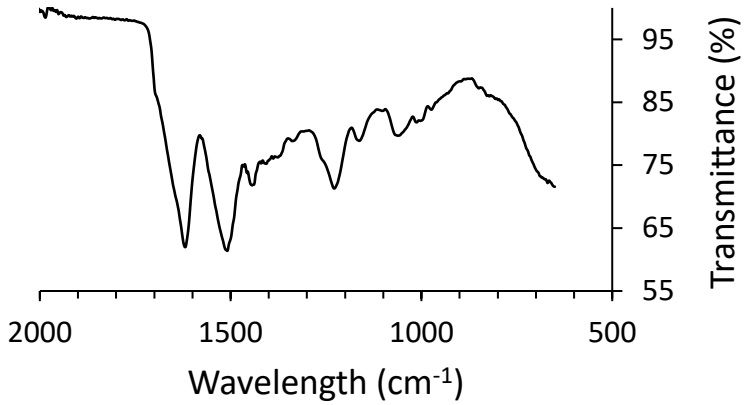

Figure 1. FT-IR spectrum of fibroin scaffold

3.2. X- ray Diffraction analysis of the silk fibroin scaffold structure

The fibroin scaffolds treated with $CaCl_2$-EtOH-H_2O showed three obvious diffraction peaks at 2θ, namely 20.6°, 24.1° and 31.4° which corresponed to crystalline spacing of 0.41 nm, 0.35 nm and 0.30 nm respectively.[4] These peaks are characteristic of amorphous/disordered silk and β-sheets.

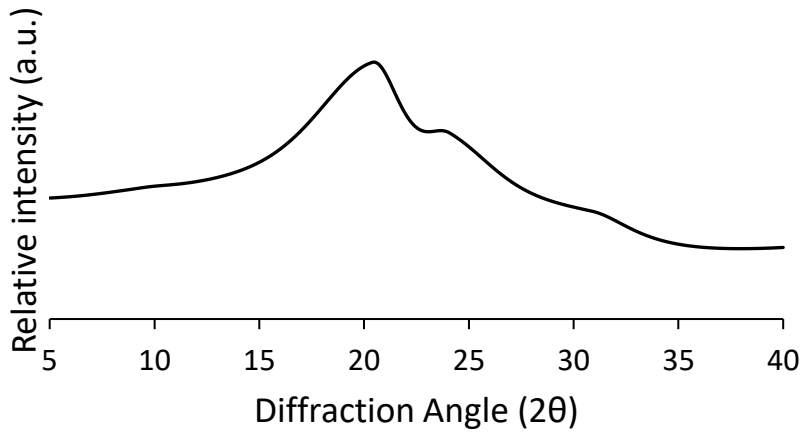

Figure 2. XRD spectrum of fibroin scaffold

3.3. Thermogravimetric analysis of the silk fibroin scaffold structure

The TGA curve (Figure 3) can be divided into three regions, each corresponding to a different mass loss rate and material phase. Region 1 is accounted for by the loss of water and occurred from 47- 170°C. Region 2, 170° C – 276°C the mass was stable. Region 3 from 276°C – 600 °C corresponds to the thermal degradation of the fibroin.[8,9]

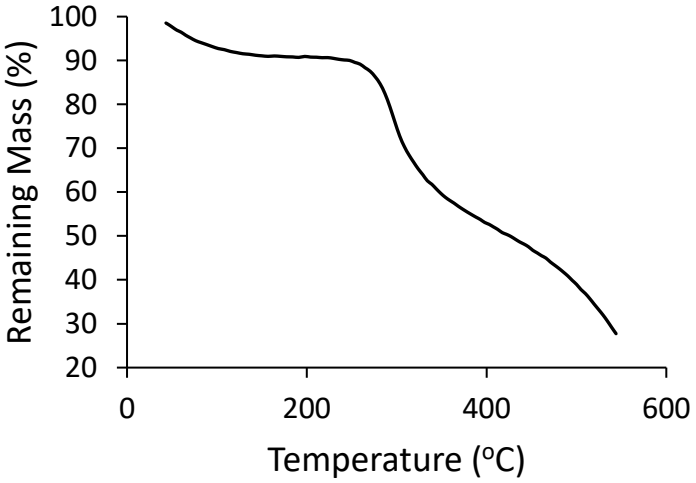

Figure 3. TGA spectrum of fibroin scaffold

3.4. Solid-state ^{13}C NMR analysis of the silk fibroin scaffold

The peaks that correspond to the amino acids that consist fibroin are presented in Figure 4 and are in agreement with the literature.[4] The presence of Ala C_B peak at 17.19 ppm corresponds to random coil or distorted β – turn and the peak at 20.30 ppm corresponds to anti-parallel β- sheets. This data confirms our findings from FT-IR studies.

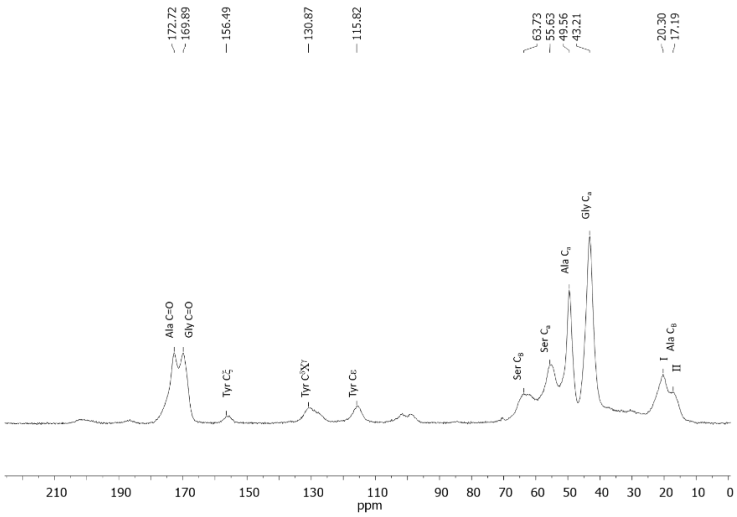

Figure 4. ssNMR spectrum of fibroin scaffold

3.5. MicroCT imaging of silk fibroin scaffold

The tomography of the sample was performed without any filter and the sample was place at the distance of 10μm from the X-ray source. The current/voltage settings used were 40kV / 181 μA. The color difference at Figure 5 is relevant to the density of the sample (darker color = higher density)

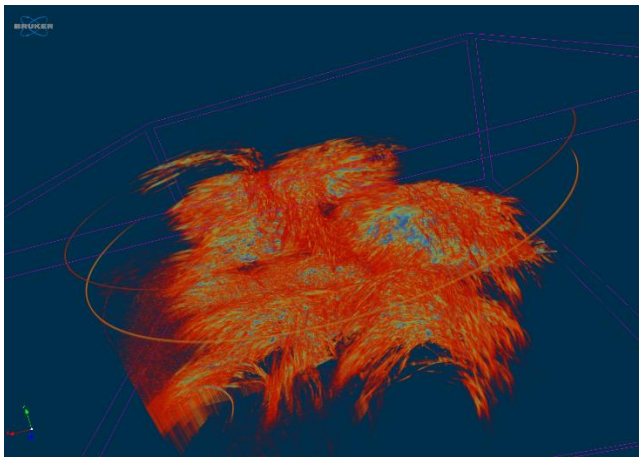

Figure 5. X-ray micro tomography of fibroin scaffold.

4. Conclusions

The ability of these scaffolds to enhance bone tissue formation via in vitro and in vivo studies is currently being assessed by the group of Xuebin Yang at the University of Leeds.

Funding: This research received no external funding.

Acknowledgments: We thank Geoff Akien for assistance with NMR, Nathan Halcovitch for assistance with XRD and Jemma Kerns for assistance with microCT.

Conflicts of Interest: The authors declare no conflict of interest.

Appendix B

All appendix sections must be cited in the main text. In the appendixes, Figures, Tables, etc. should be labeled starting with 'A', e.g., Figure A1, Figure A2, etc.

References

1. Scheibel, T. R., Hardy, J. G. & Ro, L. M. Polymeric materials based on silk proteins. *Polymer (Guildf).* **49,** 4309–4327 (2008).

2. Hardy, J. G. *et al.* Instructive Conductive 3D Silk Foam-Based Bone Tissue Scaffolds Enable Electrical Stimulation of Stem Cells for Enhanced Osteogenic Differentiation a. *Macromol. Biosci.* **15,** 1490–1496 (2015).

3. Hardy, J. G. *et al.* Biomineralization of Engineered Spider Silk Tissue Engineering. *Mater. Commun.* **9,** (2016).

4. Zhang, H. *et al.* Preparation and characterization of silk fibroin as a biomaterial with potential for drug delivery. *J. Transl. Med.* **10,** 1–9 (2012).

5. Rockwood, D. N. *et al.* Materials fabrication from Bombyx mori silk fibroin. *Nat. Protoc.* (2011). doi:10.1038/nprot.2011.379

6. Mathur, A. B., Tonelli, A., Rathke, T., Hudson, S. & State, N. C. The Dissolution and Characterization of Bombyx mori Silk Fibroin in Calcium Nitrate – Methanol Solution and the Regeneration of Films. *Biopolymers* 61–74 (1997).

7. Llang, X. I. N. & Engineering, B. Improvements of the Physical Properties of Fibroin Membranes with Sodium Alginate. *J App Polym Sci* 1937–1943 (1992).

8. Motta, A., Fambri, L. & Migliaresi, C. Regenerated Silk Fibroin Films : Thermal and Dynamic Mechanical Analysis. 1658–1665 (2002).

9. Gotoh, Y., Tsukada, M. & Minoura, N. Chemical Modification of Silk Fibroin with Cyanuric Chloride-Activated Poly (ethylene glycol): Analyses of Reaction Site by 1H-NMR Spectroscopy and Conformation of the Conjugates. *Bioconjug. Chem.* **38,** 554–559 (1993).